Alexandria Engineering Journal (2015) 54, 303–314

HOSTED BY

Alexandria University

Alexandria Engineering Journal

www.elsevier.com/locate/aej
www.sciencedirect.com

ORIGINAL ARTICLE

Performance and specific emissions contours throughout the operating range of hydrogen-fueled compression ignition engine with diesel and RME pilot fuels

Shahid Imran [a,b,*], D.R. Emberson [a], Amjad Hussain [c], Hassan Ali [d], Balazs Ihracska [f], T. Korakianitis [e]

[a] *School of Engineering and Materials Science, Queen Mary University of London, Mile End Road, E1 4NS, UK*
[b] *Department of Mechanical Engineering (KSK Campus), University of Engineering and Technology, Lahore, Pakistan*
[c] *Industrial and Manufacturing Engineering Department, University of Engineering and Technology, Lahore, Pakistan*
[d] *Department of Mechanical Engineering, Rachna College of Engineering and Technology, University of Engineering and Technology, Lahore, Pakistan*
[e] *Parks College of Engineering, Aviation and Technology, Saint Louis University, St. Louis, MO 63103, USA*
[f] *School of Engineering and Technology, University of Hertfordshire, UK*

Received 2 January 2015; revised 12 April 2015; accepted 12 May 2015
Available online 1 June 2015

KEYWORDS

Fuel map;
Thermal efficiency;
Power;
Volumetric efficiency;
Dual fuel;
Combustion

Abstract This paper presents the performance and emissions contours of a hydrogen dual fueled compression ignition (CI) engine with two pilot fuels (diesel and rapeseed methyl ester), and compares the performance and emissions iso-contours of diesel and rapeseed methyl ester (RME) single fueling with diesel and RME piloted hydrogen dual fueling throughout the engines operating speed and power range. The collected data have been used to produce iso-contours of thermal efficiency, volumetric efficiency, specific oxides of nitrogen (NO_X), specific hydrocarbons (HC) and specific carbon dioxide (CO_2) on a power-speed plane. The performance and emission maps are experimentally investigated, compared, and critically discussed. Apart from medium loads at lower and medium speeds with diesel piloted hydrogen combustion, dual fueling produced lower thermal efficiency everywhere across the map. For diesel and RME single fueling the maximum specific NO_X emissions are centered at the mid speed, mid power region. Hydrogen dual fueling produced higher specific NO_X with both pilot fuels as compared to their respective single fueling operations. The range, location and trends of specific NO_X varied significantly when compared to single fueling

* Corresponding author at: Department of Mechanical Engineering (KSK Campus), University of Engineering and Technology, Lahore, Pakistan.
E-mail address: shahidimran512@hotmail.com (S. Imran).
Peer review under responsibility of Faculty of Engineering, Alexandria University.

http://dx.doi.org/10.1016/j.aej.2015.05.007

cases. The volumetric efficiency is discussed in detail with the implications of manifold injection of hydrogen analyzed with the conclusions drawn.

Nomenclature

Abbreviations

BMEP	brake mean effective pressure
CI	compression ignition
CO	carbon mono oxide
CO_2	carbon dioxide
HC	hydrocarbons
IC	internal combustion
NO_X	oxides of nitrogen
RME	rape methyl ester
SI	spark ignition

1. Introduction

Limited reserves and the increasing environmental impact of the conventional fossil fuels have recently been two majors concerns of the researchers [1,2]. Two strategies have been evolved to meet these challenges: the use of alternate fuels to reduce the dependence on fossil fuels [3,4] and the development of clean burning fuels to meet the strict emissions targets [5]. Owing to its superior combustion characteristics, hydrogen has received particular attention [6–8].

Approximately 95% of the hydrogen currently produced is by steam reforming of natural gas (a catalytic thermo-chemical conversion process). Renewable hydrogen-production methods, such as electrolysis of water using renewably generated electricity [9], pyrolysis [10], photo-biological water splitting, photo-electro-chemical [11] water splitting, solar thermo-chemical water splitting and biomass steam gasification [12] are techniques yet to be fully realized [13] but make hydrogen a viable alternative to fossil derived fuels, or as a substitute fuel for at least a portion of the overall energy supplied to these engines, e.g. in dual fuel mode operation [14,15].

Owing to the high auto-ignition temperature of hydrogen, it is difficult to ignite a hydrogen/air mixture on the basis of mixture temperature alone. The ignition of hydrogen is achieved through a spark plug in spark ignition (SI) whereas a high cetane liquid fuel is injected at the end of compression to start the ignition in compression ignition (CI) engines. This mode of operation in CI engines is referred to as dual fueling [14,15]. Some studies have theoretically [16] and others have experimentally [17]assessed the effect of pilot fuel quantity in dual fueling mode. Studies have been conducted with diesel piloted hydrogen combustion [18] and biodiesel piloted hydrogen [14]. Comparison between these two pilots has been made [19] but at a very limited range of engine operating conditions. Also, studies [20] have indicated that the ignition delay is affected if the percentage of H_2 in fuel mixture is varied.

Hydrogen has a high burning velocity which leads to increased in-cylinder pressures and higher temperatures, resulting in increased NO_X emissions. This effect may be reduced by making the mixture leaner using hydrogen's property to be flammable over a very wide range of concentrations in air (from 4% to 75%) [21–23]. This allows for the application of learner combustion, resulting in a reduction of temperature and pressure, and lower NO_X emissions [24]. However, the initiation and development of the multiple turbulent flames require an H_2–air mixture richer than the lean flammability limit [25]. Most studies have limited the enthalpy fraction of hydrogen to a maximum of 15% [22,26]. The upper limit of hydrogen addition with manifold injected hydrogen is determined by the quenching gap of the hydrogen flame which can travel past the nearly-closed intake valve and more readily backfires into the engine's intake manifold [27]. There is a need to examine the performance and emissions of a naturally aspirated CI hydrogen dual fueled engine at higher hydrogen enthalpy fractions. The maximum enthalpy fraction in this study is 30%.

Hydrogen has been shown to increase flame stability [26] and improve thermal efficiency [28]. It is believed that the high diffusion coefficient of hydrogen leads to highly turbulent flame propagation rate [26,29,30]. The addition of hydrogen to increase the flame stability has been studied extensively because of the belief that flame propagation is the key factor in improving combustion [24,26,31,32]. Engine speed is often neglected in these studies, but it is clearly one of the key factors in mixing, flame propagation and the residence time. Increased engine speed enhances turbulence and hence affects mixing and flame propagation characteristics. On the other hand the residence time is reduced, therefore the overall effect of hydrogen addition on combustion should be examined with changing speeds. Measurement of NO_X emissions offers an indirect indication of combustion temperatures. The effect of hydrogen addition on combustion and hence the thermal efficiency with varying amounts of hydrogen has been studied previously [22,25] but often limited to one engine speed and a small range of loads.

A number of studies have examined different emissions of hydrogen in dual fueled CI engines. Some of these studies have considered engine operation at one speed only [22,25,28,33]; others have considered two speeds only [34,14]. The general trend exhibited in these studies is an increase in NO_X emissions and a decrease in HC, CO and CO_2 when compared to single fueling with their respective pilot fuels. The increase in NO_X emissions with increasing hydrogen addition are attributed to increased flame temperature, and the reductions in HC, CO

and CO_2 emissions are attributed to the reduction in the carbon content of the fuel. The range of applied loads in these studies is one [34], two [14,25] three [22], four [28] and five [33].

As discussed above, the physical as well as chemical properties of hydrogen vary significantly from the properties of the conventional fuels like gasoline and diesel. Wider flammability and non visible flames in case of hydrogen are two such properties that require additional safety measures to be taken. Regarding the design a system utilizing hydrogen as a fuel, the selection of materials used, operation, storage and transportation of hydrogen, NASA guidelines are comprehensive and useful [35].

"Fuel maps" are the performance or emissions maps presenting the full contours of thermal efficiency or brake specific fuel consumption and different specific emissions plotted throughout the power versus speed range of the engine. Only a few studies have reported such fuel maps [29,36–38]. One such study, limited to diesel and RME based single fueling, has already been conducted in the group to reflect the thermal efficiency as well as specific emissions contours on the power-speed plane [39]. Volumetric efficiency can significantly affect the performance and emissions in IC engines and has been investigated and reported [40]. In another study in the group, performance and emissions contours of natural gas fueled compression ignition engine have been presented including the effect of natural gas induction on the engine' volumetric efficiency [41]. This paper details the performance and emissions maps of a hydrogen dual fueled compression ignition engine.

The engine used in the study is a standard test rig, typical of the majority of such engines used in the developing economies of the world. The shape and region of contours in presented in this study are representative of those shapes for typical CI engines although more modern engines may have higher thermal efficiency and lower emissions.

Table 1 Engine specifications.

No. of cylinders	1
Bore	107.95 mm
Stroke	152.40 mm
Swept volume	1394×10^{-6} m^3
Clearance volume	115.15×10^{-6} m^3
Compression ratio	13.11:1
Max. power	11 kW @ 1500 r/m
IVO	10°BTDC
IVC	40°ABDC
EVO	50°BBDC
EVC	15°ATDC

2. Experimental set up

A four-stroke single-cylinder, direct-injection Gardner 1L2 compression ignition engine was used, the specifications of which are shown in Table 1. Fig. 1 shows the schematic layout of the experimental rig, which includes a hydraulic brake, fuel supply lines, various emission analyzers and instrumentation.

Pilot fuels are injected directly into the cylinder through the standard engine fuel-injection system. Hydrogen is supplied from a 20 MPa compressed hydrogen gas tank (hydrogen purity of 99.995%). A hydrogen pressure regulator fitted on the tank with a flame arrestor feeds the hydrogen fuel line at 0.15 MPa, which is connected to a hydrogen flow meter (CT Platon glass variable area flow meter, 44 l/min scale, 1.25% full scale deflection). At the control valve just before the flow meter, the pressure in the fuel line drops to about atmospheric pressure. Adjusting the hydrogen supply pressure does not affect this final supply pressure, and therefore does not affect the fuel flow rate. The hydrogen then feeds in the intake manifold via a stainless steel pipe fitted with a ball valve. This pipe is oriented such that the outlet points into the intake air stream

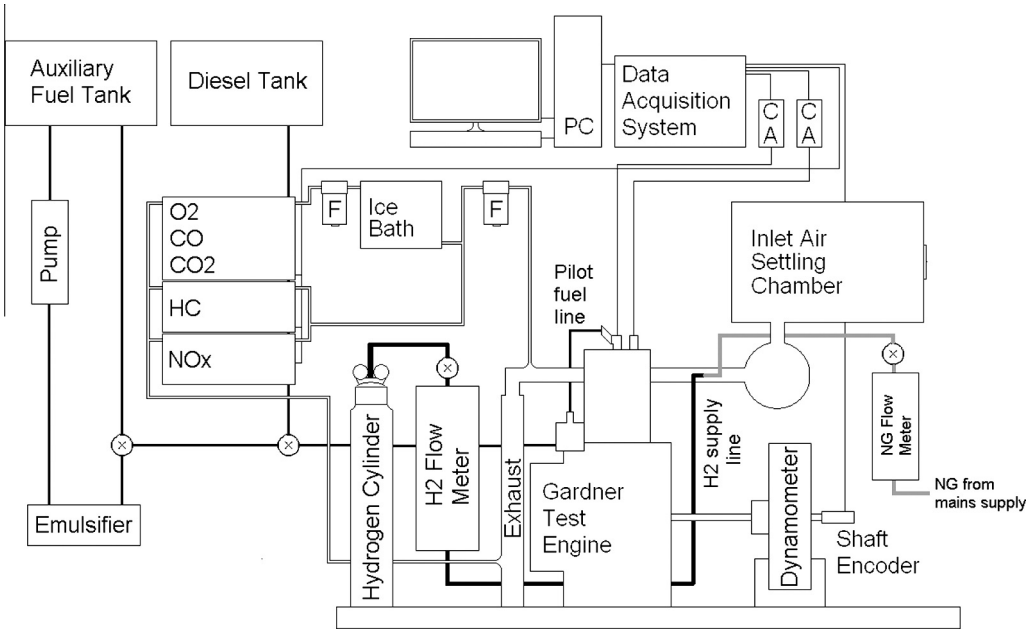

Fig. 1 Experimental rig of dual-fueled CI engine.

(against the air flow) in order to enhance mixing. Air flow measurements are made using an inclined manometer.

For the baseline diesel and RME testing, and for dual fueling, the tests were conducted at six different engine speeds, starting from 1000 rev/min and going up to 1500 rev/min with an increment of 100 rev/min. For normal CI engine operation, the load placed on the engine started at a BMEP of 0.126 MPa and went up to a BMEP of 0.630 MPa in 0.126 MPa increments. 0.630 MPa BMEP is the maximum rated load for this engine. During hydrogen dual-fuel operation the amount of pilot fuel injected is set at a flow rate providing 0.378 MPa BMEP during normal engine operation. The engine power output is then increased further by adjusting the flow rate of hydrogen inducted by the engine to reach the high load regions. Whilst operating at the highest load points the engine is unable to induct the required quantity of hydrogen to provide the power output. This is a result of manifold injection of the hydrogen and the low energy content of hydrogen on a volume basis. A consequence of this is that when the engine power output demand is high, a larger portion of the enthalpy must be met by the pilot fuel. As the pilot fuel quantity is to be kept constant during data collection this led to the pilot fuel quantity being set at a level that met the low power output demands alone, therefore hydrogen addition at the lower outputs could not be achieved, only the upper half of the standard engine load range can be achieved with hydrogen dual-fueling.

Table 2 shows the details of different analyzers used in this work to record emissions. Analyzers used to record NO_X and HC emissions were fed with sample gases through a heated line at 160 °C. Steady state operation was ensured every measurement by allowing the engine to run for 10 min. The statistical variations in measured results in steady state operation in each operating speed-power combination were insignificant, but 10 measurements were averaged at each data point. To plot the contours, the data recorded from the engine were processed and the Iso Contours of the different performance and emissions parameters were generated by using a Matlab function written for this purpose

Table 2 Analyzers used to measure different emissions.

Type of emission	Analyzer used
NO_X	Signal 4000 VM chemiluminescence analyzer
HC	Rotork analysis model 523 (FID) analyzer
CO, CO_2, O_2	Servomex 4210C

3. Sample pressure and rate of heat release data

Figs. 2(a) and (b) show in-cylinder pressure and rate of energy release for pure diesel and diesel piloted hydrogen at 0.503 MPa with diesel pilot set at 0.315 MPa for the dual fueling case 1000 rev/min. Figs. 3(a) and (b) show in-cylinder pressure and rate of energy release for pure RME and RME piloted hydrogen at 0.503 MPa with RME pilot set at 0.315 MPa for the dual fueling case 1000 rev/min. When hydrogen is piloted by either diesel RME, it produces higher peak cylinder pressure when compared to the single fueling cases based on the respective pilot fuels. Also, the rate of energy release peak is higher in case of hydrogen based dual fueling when compared to the respective single fueling cases. Pressure data were recorded and analyzed on all points and these trends are representative only and are presented to support the claims made in the following sections.

4. Diesel and diesel piloted hydrogen dual fueling

4.1. Thermal and volumetric efficiencies

Fig. 4(a) illustrates the thermal efficiency contours of the engine operating under normal CI conditions when fueled with diesel. The contours show that at any operating engine speed the engine's thermal efficiency increases with increasing power output except at the highest power levels, where a small

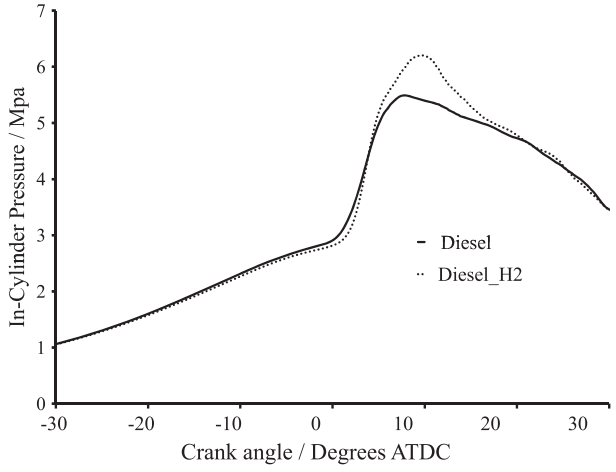

(a) Cylinder pressure for pure diesel and diesel piloted ydrogen at a BMEP of 0.503 MPa and 1000 rev/min

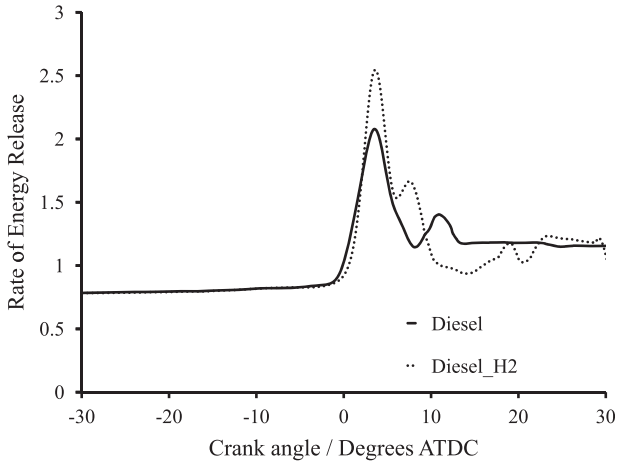

(b) Rate of energy release for pure diesel and diesel iloted hydrogen at a BMEP of 0.503 MPa and 1000 rev/min

Fig. 2 Experimentally obtained in-cylinder pressure (a) and rate of energy release (b) for pure diesel and diesel piloted hydrogen at 0.503 MPa with diesel pilot set at 0.315 MPa for the dual fueling case 1000 rev/min.

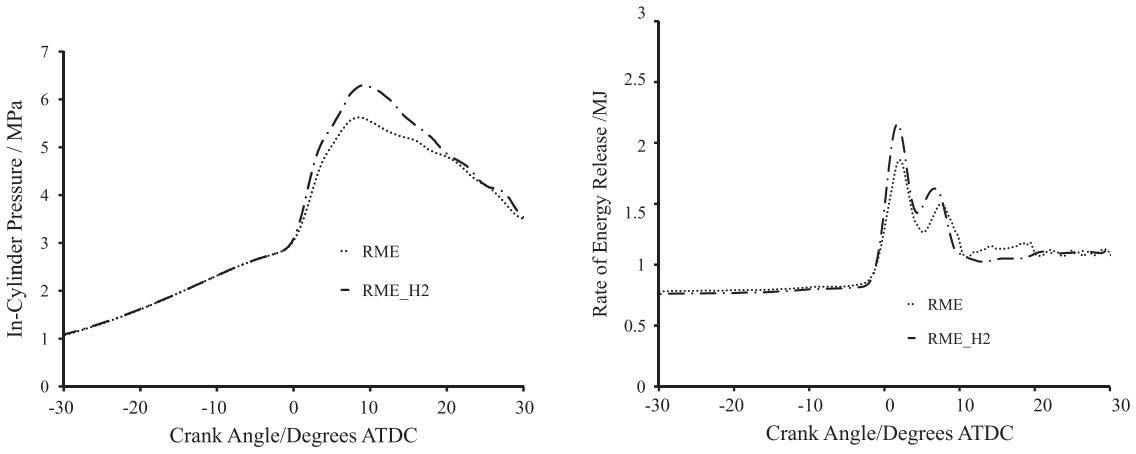

(a) Cylinder pressure for pure RME and RME piloted hydrogen at a BMEP of 0.503 MPa and 1000 rev/min

(b) Rate of energy release for pure RME and RME p iloted hydrogen at a BMEP of 0.503 MPa and 1000 rev/min

Fig. 3 Experimentally obtained in-cylinder pressure (a) and rate of energy release (b) for pure RME and RME piloted hydrogen at 0.503 MPa with diesel pilot set at 0.315 MPa for the dual fueling case 1000 rev/min.

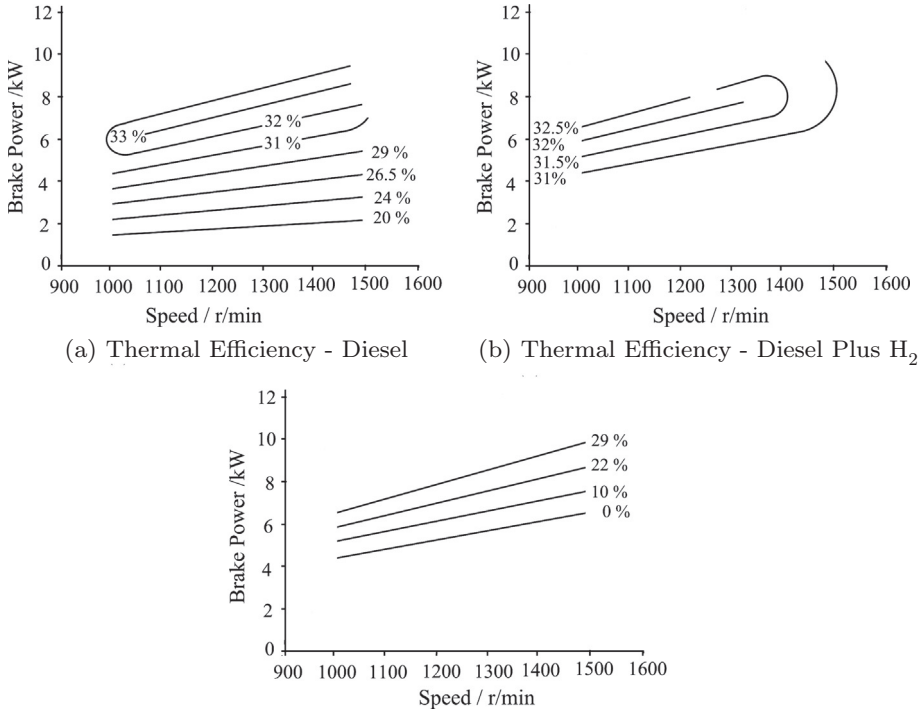

(a) Thermal Efficiency - Diesel

(b) Thermal Efficiency - Diesel Plus H_2

(c) Enthaply fraction from hydrogen

Fig. 4 Experimentally obtained thermal efficiency contours of baseline diesel (a), diesel–H_2 dual fueling operation (b) and percentage enthalpy from hydrogen in diesel–H_2 dual fueling operation (c) where in all cases the pilot fuel contributes to 0.378 MPa of the total BMEP.

reduction in thermal efficiency is observed. At the highest engine speed this reduction in thermal efficiency at the highest power is smaller. This contour plot is a good example of the advantage of expressing engine data in this manner. The full thermal efficiency contours with respect to both the power and the speed are expressed. The gradient of the contours indicates that at any value of power below 5 kW, and as engine speed increases, the thermal efficiency is monotonically decreasing. At higher engine powers, e.g. at 7 kW, the thermal efficiency is 32% at 1100 rev/min, increases to 33% at 1250 rev/min, and decreases from that maximum value with further increase in engine speeds.

The thermal efficiency contours of diesel piloted hydrogen dual fueling are shown in Fig. 4(b). They start from the

baseline low-load line with BMEP value of 0.378 MPa (where there is no hydrogen added i.e. all the fuel enthalpy is supplied by the diesel pilot fuel). Any further increase in power is obtained through the induction of hydrogen in the intake manifold, and the quantity of diesel pilot fuel is kept constant for that speed setting. The engine operates at medium and higher load conditions when it is in dual fuel operation. The maximum enthalpy fraction from hydrogen in this case is 29% as illustrated in Fig. 4(c).

In the following comparisons between the various fueling modes are made at the same speed and power settings. When a small amount of hydrogen is inducted into the intake manifold, for instance when hydrogen is contributing 10% of the total fuel enthalpy, the thermal efficiency is 1.5% lower than the standard diesel-only fuel operation as shown in Fig. 4(a). When the hydrogen enthalpy fraction was increased to 22% of the total fuel enthalpy, then the performance of the dual fuel mode deteriorated and the efficiency difference increased to 3% at the same speed and power settings. When the enthalpy fraction of H_2 was increased beyond 25% (near maximum power), it resulted in higher thermal efficiencies compared to the baseline diesel-only single fueling case at all speeds but the highest.

For different speeds while operating at a hydrogen enthalpy fraction of 29% the increase in thermal efficiency was around 1.6% (at low and medium speeds) but it was 3.0% lower at the highest speed. This is in agreement with the literature in stating that the addition of hydrogen leads to an improvement in the thermal efficiency. However, at lower power outputs there is a reduction in thermal efficiency with hydrogen addition. At the highest power outputs the higher thermal efficiency values can be attributed to hydrogen contributing to more complete combustion due to higher combustion temperatures and pressures.

Comparison of Fig. 5(a) and (b) indicates that induction of hydrogen into the intake manifold compromises volumetric efficiency by approximately 5%; but near the peak loads attainable with dual fueling there is a 1.6% increase in thermal efficiency, especially at low and medium speeds. This is because at low and medium speeds hydrogen combustion is not affected by the phenomenon of under-mixing as observed in the single fueling case (the hydrogen is inducted into the intake manifold and it has more time to mix with air). This could be an advantage of manifold induction over direct injection of hydrogen into the combustion chamber.

In general, at a given power rating the volumetric efficiency decreases as the engine speed increases due to increasing friction of the airflow during the induction and exhaust phase of the cycle. At a given engine operating speed higher loads mean more fuel and higher operating temperatures, including higher inlet manifold temperature, thus heating the intake air and adding to the reduction volumetric efficiency. Comparison of Fig. 5(a) and (b) illustrates that the slope of the volumetric efficiency contours is flatter for hydrogen dual fueling than for baseline diesel operation. The lower values are observed because in the dual-fueling case, a part of the incoming air is being displaced by the hydrogen in the intake manifold, thus reducing the air flow rate. The frictional losses are known to increase as the square of engine speed [38]. The slope of the iso-contours of volumetric efficiency for dual fuel mode differ significantly from those for single fuel mode. This is due to a larger portion of the intake air being displaced by the increasing addition of the hydrogen as the engine speed is increased. This increasing amount of displacement leads to a difference in scaling of volumetric efficiency with engine speed between the two modes. This is another consequence of the addition of the hydrogen in the intake manifold. As the volumetric efficiency is calculated from the air flow rate, increasing levels of hydrogen at the manifold displace air from the flow rate. There is less air flowing through the intake system thus the frictional effects of speed are reduced leading to the variation in scaling that is observed in the single fueling case.

The volumetric efficiency map as shown in Fig. 5(b) reflects the lower values for the dual fuel mode. This is to be expected as a portion of the inducted air is being displaced by the hydrogen in the intake, reducing the air partial pressure below that of the mixture pressure. Also as to be expected is the drop of volumetric efficiency as the engine speed increases for both modes of operation. This drop in volumetric efficiency between the two modes is clear when Fig. 5(a) and (b) are compared.

4.2. Specific NO_X

Fig. 6(a) shows the full contours of specific NO_X emissions for the engine operating on baseline diesel fuel. The absolute value of NO_X emissions is increasing with increasing combustion temperature and increasing residence time. Therefore as engine operating speed is increases NO_X emissions increase up to a maximum in mid operating speed, and then decrease as

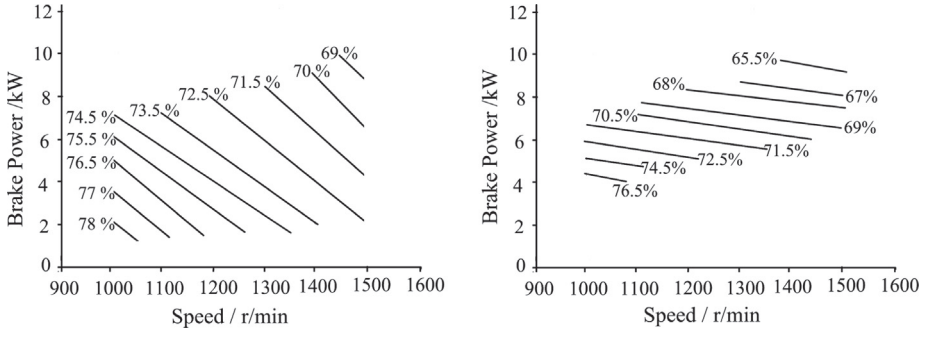

(a) Volumetric Efficiency - Diesel (b) Volumetric Efficiency - Diesel Plus H_2

Fig. 5 Experimentally obtained volumetric efficiency contours of baseline diesel (a) and diesel–H_2 dual fueling operation (b) where in all cases the pilot fuel contributes to 0.378 MPa of the total BMEP.

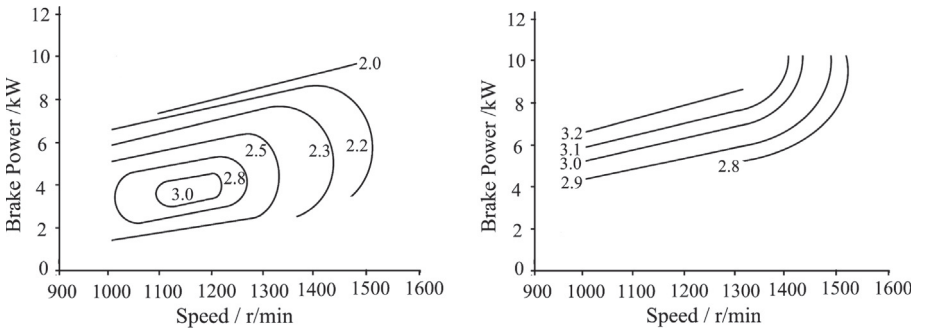

(a) Specific NO_X /g/MJ - Diesel (b) Specific NO_X /g/MJ - Diesel Plus H_2

Fig. 6 Experimentally obtained specific NO_X emissions contours for baseline diesel (a) and diesel–H_2 dual fueling (b).

residence time decreases with increasing rev/min. At any engine operating speed the absolute NO_X emissions increase with increasing power, but after the mid-power range the increase in absolute NO_X is lower than the increase in power, so that the specific NO_X emissions decrease above the mid-power range. These combined effects result in a central region of maximum specific NO_X in the power-speed plane. At constant speed as the power output is increased or decreased from this central region, the specific NO_X decreases. Similarly, at constant power as the speed is increased or decreased past the central region, the specific NO_X decreases.

Fig. 6(b) reflects the higher NO_X specific emissions in the diesel–hydrogen dual-fueling case. Compared to the baseline diesel fueling, hydrogen based dual fueling resulted in higher NO_X at all speed and power combinations. The high diffusivity (ability to disperse in the air) of hydrogen makes the combustible mixture more pre-mixed, hence improving the combustion quality, resulting in higher in-cylinder temperatures. Smaller quenching distance in the case of hydrogen can be another reason for these higher specific NO_X emissions. Smaller quenching distances make it possible for the hydrogen flame to travel closer to the combustion chamber walls before being extinguished, maintaining higher temperatures longer in the end phases of the combustion process. The range of specific NO_X values is in a narrow band between 2.8 and 3.2 g/MJ across operating speeds and powers. This can be attributed to insignificant variation in minimum ignition energy required when the equivalence ratio varies in range $0.5 < \phi < 1.0$, leading in earlier beginning of combustion and therefore in higher in-cylinder temperature and pressure.

The slightly lower specific NO_X values at higher speeds can be attributed to the shorter residence time available. The specific NO_X values reflect three parameters: the in-cylinder temperature; the oxygen available; and the efficiency of the engine (a result of the specific nature of the measurement). As the power increases at constant speed, higher absolute NO_X results due to higher in-cylinder temperature, and at the same time the engine is becoming more efficient. At higher powers, the rate at which the in-cylinder temperature increases is dominated by the rate at which the engine efficiency increases with any changes in the load applied to the engine. Therefore, the lower ignition energy and wider operating equivalence ratio of hydrogen result in the specific NO_X trends in the diesel–hydrogen fueling case to follow the shape of the thermal efficiency contours.

4.3. Specific HC

For the baseline single-fuel diesel case the specific HC emissions shown in Fig. 7(a) follow the reverse of the thermal efficiency contour shapes. Thus the lowest values of the specific HC emissions are in the regions of the highest thermal efficiency contours, and the high specific HC emissions are measured at the lower power outputs. The specific HC emissions map for diesel piloted hydrogen dual-fuel mode is shown in Fig. 7(b).

The specific HC emissions follow similar trends (they follow the reverse of the thermal efficiency contours of the dual-fueling case). Overall at the same speed and power settings

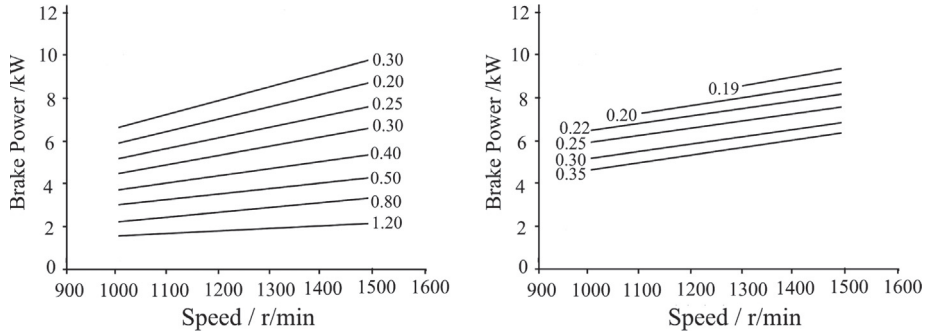

(a) Specific HC /g/MJ - Diesel (b) Specific HC /g/MJ - Diesel Plus H_2

Fig. 7 Experimentally obtained specific HC emissions contours for baseline diesel (a) and diesel–H_2 dual fueling (b).

the specific HC emissions are slightly lower in the dual fuel mode compared to the baseline diesel single-fuel case.

This is because the amount of carbon going into the engine is not increasing as the pilot fuel quantity is fixed at the base load setting. Better combustion at higher load due to higher in-cylinder temperature can be another reason for this significant decrease in specific HC. This shows that unlike diesel, diesel ignited H_2 combustion does not have the problem of under mixing at higher loads. Fig. 4(b) illustrates that at the highest power with the enthalpy fraction of hydrogen at 29%, the dual fueling case is more efficient compared to single fueling at the same operating points. This demonstrates a higher combustion efficiency as well as producing more brake power. This is another reason for the reduction of the HC emissions. Fundamental studies of non-premixed combustion have shown increased flame stability due to higher flame speeds and improved mixing with the increased hydrogen addition [26]. The results presented here are consistent with this argument. Although the volumetric efficiency of the dual fueling case is about 5% less than diesel based single fueling, the specific HC values are lower. This can be attributed to better mixing of the hydrogen and air, the lower carbon content in the mixture, and the faster reaction rates of hydrogen combustion.

4.4. Specific CO_2

Figs. 8(a) and (b) show specific CO_2 maps for the baseline diesel and the diesel piloted dual fueling of hydrogen respectively. Diesel piloted hydrogen combustion produces less CO_2 when compared to the pure diesel based single fueling. When the hydrogen fraction is 22% and 29%, a decrease of 12.5% and 35% in CO_2 is observed. When compared to diesel based normal fueling, lower values of CO_2 emissions can be attributed to the lower carbon to hydrogen ratio. About a 5% loss in volumetric efficiency can be another reason for this but the specific O_2 map for the dual fueling as shown in Fig. 8(c) does not support this argument. Similar levels of specific O_2 are observed both for the single as well as the dual fueling case. This also shows that the improved combustion of hydrogen can compensate for the oxygen which is displaced by the injection of hydrogen into the intake manifold.

5. RME and RME piloted hydrogen dual fueling

5.1. Thermal and volumetric efficiencies

Fig. 9(a) illustrates the thermal efficiency contours of the engine operating under normal CI conditions when fueled with RME. Overall the shape of the thermal efficiency contours for diesel and RME baselines are very similar, but the thermal efficiency with RME is marginally higher than with diesel. The thermal efficiency contours with hydrogen dual fueling and RME pilot fuel are shown in Fig. 9(b).

They start from the baseline low-load line with BMEP value of 0.378 MPa (where there is no hydrogen added i.e. all the fuel enthalpy is supplied by the RME pilot fuel). Any further increase in power is obtained through the induction of hydrogen in the intake manifold, and the quantity of RME pilot fuel is kept constant for that speed setting. The engine operates at medium and higher load conditions when it is in dual fuel operation. The maximum enthalpy fraction from hydrogen in this case is 33% as illustrated in Fig. 9(c).

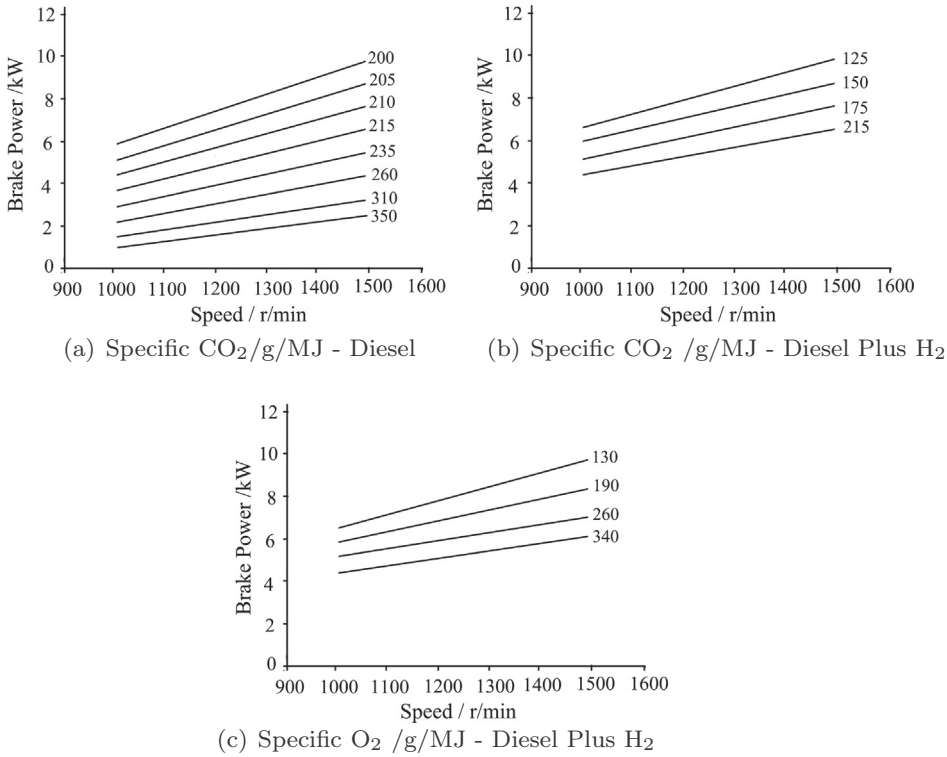

(a) Specific CO_2/g/MJ - Diesel

(b) Specific CO_2 /g/MJ - Diesel Plus H_2

(c) Specific O_2 /g/MJ - Diesel Plus H_2

Fig. 8 Experimentally obtained specific CO_2 emissions contours for baseline diesel (a) and diesel–H_2 dual fueling (b) and specific O_2 emissions for diesel–H_2 dual fueling (c).

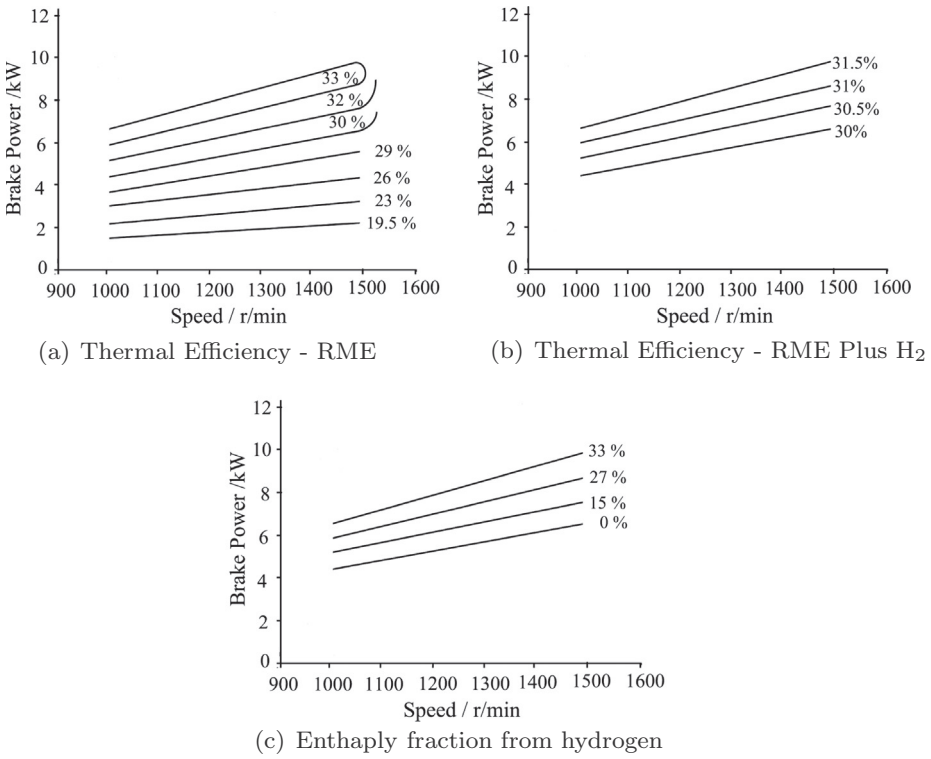

(a) Thermal Efficiency - RME

(b) Thermal Efficiency - RME Plus H_2

(c) Enthaply fraction from hydrogen

Fig. 9 Experimentally obtained thermal efficiency contours of baseline RME (a), RME–H_2 dual fueling operation (b), and percentage enthalpy from hydrogen in RME–H_2 dual fueling operation (c) where in all cases the pilot fuel contributes to 0.378 MPa of the total BMEP.

Similarly to the diesel-pilot case, the engine is operating at high medium and high power conditions when it is fueled by RME-piloted hydrogen. Comparison of Fig. 9(a) and (b) illustrates that the thermal efficiency has deteriorated with the addition of hydrogen, and the deterioration is slightly higher than what is observed in the diesel piloted hydrogen dual fueling case. When 15%, 27% and 33% of the total enthalpy is provided by hydrogen, the thermal efficiency of this dual fueling case decreases by about 5% for all cases at all speeds. Similar differences are observed when diesel piloted hydrogen combustion is compared to RME piloted hydrogen combustion. From the thermal efficiency point of view diesel has proved to be better pilot fuel compared to RME. More hydrogen is inducted when RME is used to pilot the hydrogen combustion. The performance comparison of diesel and RME as pilot fuels is shown in Table 3. The inferior performance of RME as a pilot fuel can be attributed to its poor ignition characteristics. The table shows hydrogen enthalpy fraction against any improvement or deterioration in thermal efficiency and specific NO_X. The thermal efficiency and NO_X columns contain percentage change in these parameters when compared to the respective single fueling cases with diesel and RME as baselines.

The slopes and values of volumetric efficiency contours for diesel and RME baseline cases as shown in Figs. 5 and 10(a) are very similar. The slope of the volumetric efficiency contours for RME piloted combustion of hydrogen as shown in Fig. 10(b) is flatter than the slope of the volumetric efficiency contours for diesel piloted hydrogen as shown in Fig. 5(b).

Table 3 Performance comparison of diesel and RME as pilot fuels in hydrogen combustion.

Pilot fuel	Load/speed	Enthalpy fraction of H_2	Thermal efficiency	Specific NO_X
Diesel	Lower medium/all	10%	1.5%↓	3.3%↑
	Medium/ low → medium	22%	3.2%↓	16%↑
	High/ low → medium	29%	1.5%↑	31%↑
	High/high	29%	3.2%↑	27%↑
RME	Lower medium/all	15%	4.5%↓	4%↑
	Medium/all	27%	6%↓	7%↑
	High/all	33%	4.5%↓	23%↑

This is a consequence of the reduced heating value of RME compared to diesel. Figs. 4 and 9(c) show the enthalpy contribution of hydrogen for diesel and RME piloted dual fueling of hydrogen. The enthalpy fraction of hydrogen at each setting is larger with RME as compared to the diesel dual fueling hence a larger proportion of the intake air is being displaced by the hydrogen, further increasing the change in scaling between speed and volumetric efficiency as discussed previously at the end of Section 4.1.

5.2. Specific NO_X

Figs. 11(a) and (b) illustrate the specific NO_X contours for the RME baseline and the RME piloted dual fueling of hydrogen respectively. The overall trends and explanations for the specific NO_X emissions with RME single fueling are analogous to those of baseline diesel and diesel-piloted hydrogen of the previous section.

Comparison of Fig. 11(a) and (b) reflects an overall higher NO_X with RME piloted hydrogen combustion when compared to the RME single fueling case.

The RME piloted hydrogen combustion results in higher absolute NO_X due to higher in-cylinder temperatures. In addition the comparison of the thermal efficiency contours suggests that the RME piloted dual fueling is less efficient compared to pure RME single fueling across the entire contour range. When the two dual fueling cases are compared in terms of specific NO_X emissions, RME piloted hydrogen combustion produces lower specific NO_X compared to the diesel based dual fueling. Reduced volumetric efficiency in case of RME piloted hydrogen combustion when compared to the diesel based dual fueling case can be a reason for lower NO_X.

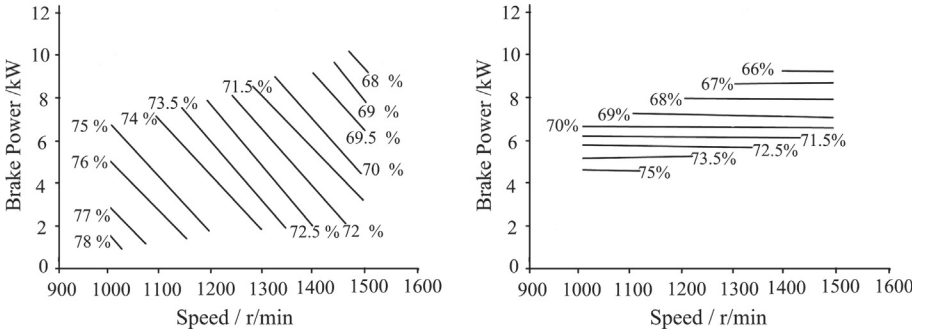

(a) Volumetric Efficiency - RME (b) Volumetric Efficiency - RME Plus H_2

Fig. 10 Experimentally obtained volumetric efficiency contours of baseline RME (a) and RME–H_2 dual fueling operation (b) at constant pilot fuel BMEP of 0.378 MPa.

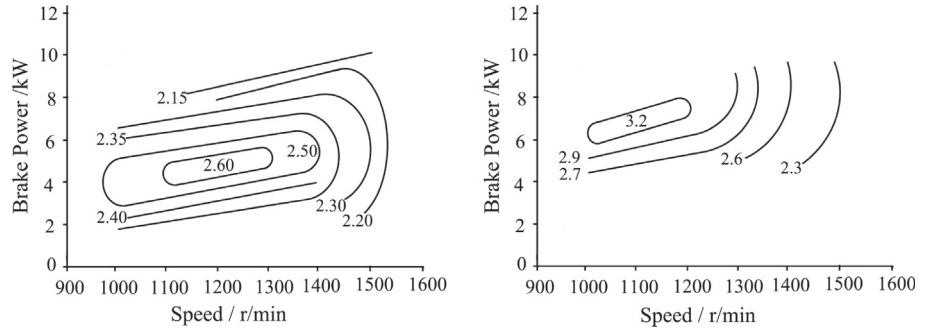

(a) Specific NO_X /g/MJ - RME (b) Specific NO_X /g/MJ - RME Plus H_2

Fig. 11 Experimentally obtained specific NO_X emissions contours for RME baseline (a) and RME–H_2 dual fueling (b).

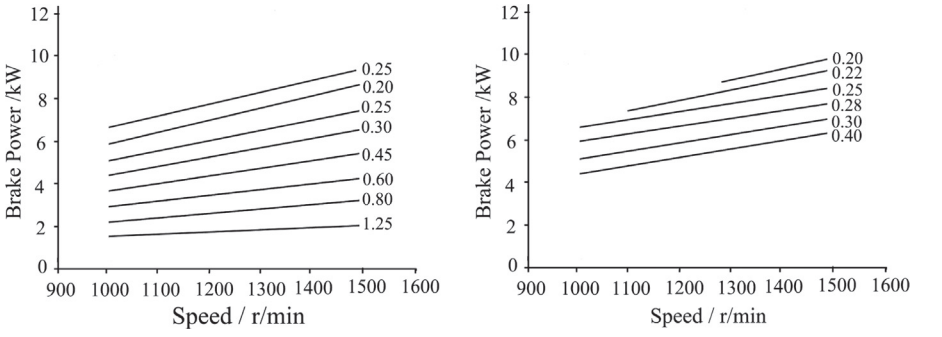

(a) Specific HC /g/MJ - RME (b) Specific HC /g/MJ - RME Plus H_2

Fig. 12 Experimentally obtained specific HC emissions contours for RME baseline (a) and RME–H_2 dual fueling (b).

5.3. Specific HC

Figs. 12(a) and (b) illustrate the specific HC maps for the RME baseline and the RME piloted dual fueling of hydrogen respectively. The overall trends and explanations for specific HC emissions with RME single fueling and RME piloted dual fueling of hydrogen are analogous to those of baseline diesel and diesel-piloted hydrogen of the previous section. Similar or slightly higher specific HC values are recorded when RME substitutes diesel for piloted hydrogen combustion. This small difference in specific HC numbers can be attributed to the relatively poor atomization and ignition characteristics of RME compared to diesel for the similar roles.

Although more carbon is being injected at higher power outputs, in the case of single fueling the specific HC values for both modes (single and dual) are practically the same. Fig. 9(a) and (b) that illustrate the thermal efficiency contours for the two modes can be used to explain this trend. As discussed earlier, RME based single fueling is shown to be more efficient compared to RME piloted hydrogen dual fueling. This results in more brake power thus reducing the magnitude of specific HC emissions despite the fact that the absolute values of HC are higher.

6. Conclusions

Many studies presenting performance and emissions characteristics of CI engines operating with various fuels, including hydrogen, present these characteristics at a few load settings and engine rotational speed combinations. With hydrogen fueled CI engines these studies are usually limited to one type of pilot fuel (in most cases diesel). Few studies are available where different types of pilot fuels have been investigated with hydrogen; and in general engine performance and emissions contours have not been investigated throughout the operating speed and power range. In the work presented here the performance and emissions contours of a hydrogen fueled CI engine with two pilot fuels (diesel and RME) are experimentally investigated, assessed, compared, and critically discussed.

- In single fuel mode diesel and RME behave very similarly. The maximum thermal efficiency reached with RME is marginally higher than the maximum thermal efficiency reached with diesel. The specific NO_X emissions contours have similar trends, and those with RME are higher than those with diesel.
- In dual fuel mode the maximum thermal efficiency reached with RME is marginally lower than the maximum thermal efficiency reached with diesel. The specific NO_X emissions contours have similar trends, and those with RME are lower than those with diesel.
- In general, at a given power rating the volumetric efficiency decreases as the engine speed increases due to increasing friction of the airflow during the induction and exhaust phase of the cycle. At a given engine operating speed higher loads mean more fuel and higher operating temperatures, including higher inlet manifold temperature, thus heating the intake air and reducing volumetric efficiency. The slope of the volumetric efficiency contours is flatter and values are lower for hydrogen dual fueling when compared to diesel and RME based single fueling cases. This is a consequence of the method used to introduce hydrogen into the engine. As the hydrogen has been introduced via manifold injection, a portion of the intake air is displaced by the hydrogen, reducing the measured volume flow rate of air into the engine. This leads to a reduction of the engine's volumetric flow rate. The slope of the iso-contours differs due to a change in the scaling of volumetric efficiency with engine speed. As the amount of hydrogen added is increased to meet the increase in speed demand, larger amounts of air are displaced. As the hydrogen is introduced at the manifold and does not flow through the entire intake system but the air does, the scaling law as noted by Heywood [38] does not hold.
- For diesel and RME single fueling the location of maximum NO_X is in the central region of the maps, with the specific NO_X decreasing in all directions across the whole map. For low and medium speeds, the specific NO_X emissions increase initially as the power output is increased, and then start to decrease after reaching a maximum value. RME produces lower specific NO_X as compared to the diesel fuel.
- The hydrogen addition has been shown to increase specific NO_X emissions with both of the pilot fuels when compared to the respective single fueling cases. The lower ignition energy and wider operating equivalence ratio of hydrogen result in the specific NO_X trends in the diesel piloted dual fueling to follow the shape of the thermal efficiency contours.
- RME piloted hydrogen shows slightly reduced NO_X emissions compared to diesel piloted hydrogen at higher speeds.
- Lower specific HC emissions were recorded at highest loads attributed to reduction in carbon–hydrogen ratio and improved combustion with increasing hydrogen addition.
- Overall diesel has shown better performance as a pilot fuel for hydrogen.

Acknowledgement

We thank Steve Warren of BP Marine Ltd (Fuels) UK for coordinating the donation of the RME used in this work.

References

[1] D. Hansdah, S. Murugan, L.M. Das, Experimental studies on a DI diesel engine fueled with bioethanol–diesel emulsions, Alex. Eng. J. 52 (2013) 267–276.
[2] R.J. Crookes, T. Korakianitis, A.M. Namasivayam, A systematic experimental assessment of the use of rapeseed methyl ester (RME) as a compression ignition engine fuel during conventional and dual-fuel operation, in: TAE 7th International Colloquium on Fuels, Stuttgart, 14–15 January 2009.
[3] R.J. Crookes, K.D.H. Bob-Manuel, RME or DME: a preferred alternative fuel option for future diesel engine operation, Energy Convers Manage. 48 (11) (2007) 2971–2977.
[4] J.S. Basha, R.B. Anand, Performance, emission and combustion characteristics of a diesel engine using Carbon Nanotubes blended Jatropha Methyl EsterEmulsions, Alex. Eng. J. 53 (2014) 259–273.
[5] A. Eveleigh, N. Ladommatos, R. Balachandran, A. Marca, Conversion of oxygenated and hydrocarbon molecules to particulate matter using stable isotopes as tracers, Combust. Flame 161 (2014) 2966–2974.

[6] C.D. Rakopoulos, C.N. Michos, Generation of combustion irreversibilities in a spark ignition engine under biogas hydrogen mixtures fueling, Int. J. Hydrogen Energy 34 (10) (2009) 4422–4437.
[7] C.G. Fotache, T.G. Kreutz, C.K. Law, Ignition of hydrogen-enriched methane by heated air, Combust. Flame 110 (1997) 429–440.
[8] B.C. Choi, S.H. Chung, Autoignited laminar lifted flames of methane/hydrogen mixtures in heated coflow air Combust, Flame 159 (2011) 1481–1488.
[9] B. Olateju, J. Monds, A. Kumar, Large scale hydrogen production from wind energy for the upgrading of bitumen from oil sands, Appl. Energy 118 (0) (2014) 48–56.
[10] R. Prakash, R.K. Singh, S. Murugan, Experimental studies on combustion, performance and emission characteristics of diesel engine using different biodiesel bio oil emulsions, J. Energy Inst., http://dx.doi.org/10.1016/j.joei.2014.04.005.
[11] Y.R. He, F.F. Yan, H. Q Yu, S.J. Yuan, Z.H. Tong, G.P. Sheng, Hydrogen production in a light-driven photoelectrochemical cell, Appl. Energy 113 (0) (2014) 164–168.
[12] A. Makaruk, M. Miltner, M. Harasek, Membrane gas permeation in the upgrading of renewable hydrogen from biomass steam gasification gases, Appl. Therm. Eng. 43 (2012) 134–140.
[13] J. Ohi, Hydrogen energy cycle: an overview, J. Mater. Res. 20 (12) (2005) 3180–3187.
[14] T. Korakianitis, A.M. Namasivayam, R.J. Crookes, Hydrogen dual-fuelling of compression ignition engines with emulsified biodiesel as pilot fuel, Int. J. Hydrogen Energy 35 (24) (2010) 13329–13344.
[15] T. Korakianitis, A.M. Namasivayam, R.J. Crookes, Natural-gas fuelled spark-ignition (SI) and compression-ignition (CI) engine performance and emissions, Prog. Energy Combust. 37 (1) (2011) 89–112.
[16] R.G. Papagiannakis, P.N. Kotsiopoulos, T.C. Zannis, E.A. Yfantis, D.T. Hountalas, C.D. Rakopoulos, Theoretical study of the effects of engine parameters on performance and emissions of a pilot ignited natural gas diesel engine, Energy 35 (2) (2010) 1129–1138.
[17] S. Imran, D.R. Emberson, B. Ihracska, D.S. Wen, R.J. Crookes, T. Korakianitis, Effect of pilot fuel quantity and type on performance and emissions of natural gas and hydrogen based combustion in a compression ignition engine, Int. J. Hydrogen Energy 39 (10) (2014) 5163–5175.
[18] M.M. Roy, E. Tomita, N. Kawahara, Y. Harada, A. Sakane, An experimental investigation on engine performance and emissions of a supercharged H_2–diesel dual-fuel engine, Int. J. Hydrogen Energy 35 (2) (2010) 844–853.
[19] T. Korakianitis, A.M. Namasivayam, R.J. Crookes, Diesel and rapeseed methyl ester (rme) pilot fuels for hydrogen and natural gas dual-fuel combustion in compression-ignition engines, Fuel 90 (7) (2011) 2384–2395.
[20] C. Tang, X. Man, L. Wei, L. Pan, Z. Huang, Further study on the ignition delay times of propanehydrogenoxygenargon mixtures: effect of equivalence ratio, Combust. Flame 160 (2013) 2283–2290.
[21] Z. Huang, Y. Zhang, K. Zeng, B. Liu, Q. Wang, D. Jiang, Measurements of laminar burning velocities for natural gashydrogenair mixtures Combust, Flame 146 (2006) 302–311.
[22] V. Edwin Geo, G. Nagarajan, B. Nagalingam, Studies on dual fuel operation of rubber seed oil and its bio-diesel with hydrogen as the inducted fuel, Int. J. Hydrogen Energy 33 (21) (2008) 6357–6367.
[23] M.M. Roy, E. Tomita, N. Kawahara, Y. Harada, A. Sakane, Performance and emission comparison of a supercharged dual-fuel engine fueled by producer gases with varying hydrogen content, Int. J. Hydrogen Energy 34 (18) (2009) 7811–7822.
[24] A. Tsolakis, A. Megaritis, Catalytic exhaust gas fuel reforming for diesel engines: effects of water addition on hydrogen production and fuel conversion efficiency, Int. J. Hydrogen Energy 29 (13) (2004) 1409–1419.
[25] T. Gatts, H. Li, C. Liew, S. Liu, T. Spencer, S. Wayne, N. Clark, An experimental investigation of H_2 emissions of a 2004 heavy-duty diesel engine supplemented with H_2, Int. J. Hydrogen Energy 35 (20) (2010) 11349–11356.
[26] G.P. McTaggart-Cowan, S.N. Rogak, S.R. Munshi, P.G. Hill, W.K. Bushe, Combustion in a heavy-duty direct-injection engine using hydrogen–methane blend fuels, Int. J. Engine Res. 10 (1) (2009) 1–13.
[27] P.G. Aleiferis, M.F. Rosati, Flame chemiluminescence and oh LIF imaging in a hydrogen-fuelled spark-ignition engine, Int. J. Hydrogen Energy 37 (2) (2012) 1797–1812, 10th International Conference on Clean Energy 2010.
[28] P.K. Bose, D. Maji, An experimental investigation on engine performance and emissions of a single cylinder diesel engine using hydrogen as inducted fuel and diesel as injected fuel with exhaust gas recirculation, Int. J. Hydrogen Energy 34 (11) (2009) 4847–4854.
[29] R. Owston, J. Abraham, Structure of hydrogen triple flames and premixed flames compared, Combust. Flame 157 (2012) 1552–1565.
[30] S. Palle, R.S. Miller, Analysis of high-pressure hydrogen, methane, and heptane laminar diffusion flames: thermal diffusion factor modeling, Combust. Flame 151 (2007) 581–600.
[31] A. Tsolakis, A. Megaritis, Partially premixed charge compression ignition engine with on-board production by exhaust gas fuel reforming of diesel and biodiesel, Int. J. Hydrogen Energy 30 (7) (2005) 731–745.
[32] A. Tsolakis, A. Megaritis, D. Yap, Application of exhaust gas fuel reforming in diesel and homogeneous charge compression ignition (hcci) engines fuelled with biofuels, Energy 33 (3) (2008) 462–470.
[33] N. Saravanan, G. Nagarajan, K. M Kalaiselvan, C. Dhanasekaran, An experimental investigation on hydrogen as a dual fuel for diesel engine system with exhaust gas recirculation technique, Renew. Energy 33 (3) (2008) 422–427.
[34] G.K. Lilik, H. Zhang, J.M. Herreros, D.C. Haworth, A.L. Boehman, Hydrogen assisted diesel combustion, Int. J. Hydrogen Energy 35 (9) (2010) 4382–4398.
[35] NASA Safety Standards for Hydrogen and Hydrogen Systems, Guidelines for Hydrogen System Design, Material Selection, Operation, Storage and Transportation, NSS 1740.16.1997.
[36] C.R. Ferguson, A.T. Kirkpatrick, Internal Combustion Engines, Applied Thernal Sciences, John Wiley and Sons, Inc, 2001.
[37] R. Stone, Introduction to Internal Combustion Engines, The Macmillan Press Ltd, London, 1985.
[38] J.B. Heywood, Internal Combustion Engine Fundamentals, McGraw-Hill, New York, 1988.
[39] S. Imran, D.R. Emberson, D.S. Wen, A. Diez, R.J. Crookes, T. Korakianitis, Performance and specific emissions contours of a diesel and {RME} fueled compression-ignition engine throughout its operating speed and power range, Appl. Energy 111 (0) (2013) 771–777.
[40] Y.S.H. Najjar, O.H. Ghazal, K.J.M. AL-Khishali, Performance improvement of green cars by using variable-geometry engines, J. Energy Inst., http://dx.doi.org/10.1016/j.joei.2014.03.017.
[41] S. Imran, D.R. Emberson, A. Diez, D.S. Wen, R.J. Crookes, T. Korakianitis, Natural gas fueled compression ignition engine performance and emissions maps with diesel and {RME} pilot fuels, Appl. Energy 124 (2014) 354–365.